

# Badminton-like LiCoPO<sub>4</sub> Nanomaterials: Synthesis, Characterization and Electrochemical Performance as Lithium-Ion Battery Cathodes

Sheng-Xuan LIN<sup>a</sup>, Xiao-Gang WEN<sup>b\*</sup> and Wei QIN<sup>c</sup>

School of Material Science and Engineering, Sichuan University, Chengdu, 610065, P. R. China

<sup>a</sup>linshengxuan1688@126.com

<sup>b</sup>wenxg@scu.edu.cn

<sup>c</sup>gzdyqw@163.com

**Keywords:** LiCoPO<sub>4</sub>, Badminton-like, Nanomaterials, Lithium ion battery

**Abstract.** Badminton-like LiCoPO<sub>4</sub> nanomaterials were synthesized by a hydrothermal method, using PEG 200 as the structure directing agent, followed by a high temperature post annealing process. LiCoPO<sub>4</sub> nanoparticles could be obtained when PEG 200 is absent during the same synthesis process. As-synthesized products were characterized using X-ray diffraction (XRD), scanning electron microscopy (SEM), transmission electron microscopy (TEM). Lithium ion battery performance of synthesized LiCoPO<sub>4</sub> nanobadminton was also measured. The initial discharge capacities of LiCoPO<sub>4</sub> can reach 132.4 mAhg<sup>-1</sup> at 0.1C. After 50 cycles, the discharge capacity has been decreased to 99.6 mAhg<sup>-1</sup> and the capacity retention is about 75.2%. The electrochemical performance of LiCoPO<sub>4</sub> nanobadminton is better than LiCoPO<sub>4</sub> nanoparticles synthesized in the absence of PEG 200 and many other LiCoPO<sub>4</sub> materials reported in the literature. The excellent electrochemical performance of LiCoPO<sub>4</sub> nanobadminton can be attributed to its unique badminton-like nanostructures consisted of many long and thin nanorods.

## Introduction

Since Padhi et al. [1] first proposed the use of olivine-structured LiMPO<sub>4</sub> (M= Fe, Mn, Co and Ni) as cathodes for lithium-ion batteries in 1997, LiMPO<sub>4</sub> has been widely investigated. LiCoPO<sub>4</sub> has a reasonable operating potential of 4.8V vs. Li<sup>+</sup>/Li and high theoretical capacity of 167mAhg<sup>-1</sup>. It enables LiCoPO<sub>4</sub> to deliver a specific energy density as large as 800 Whkg<sup>-1</sup>, which is 430% more than the commercialized isostructural LiFePO<sub>4</sub> cathode material [2]. However, LiCoPO<sub>4</sub> shows a poor rate capacity and short cycle life due to its low electronic [3, 4] and ion conductivity [5], side reaction between active material and electrolyte [6,7]. Various strategies including metal ion doping [8,9], coating with electronically conducting agents [10,11], and particle size reduction [12,13] have been developed to improve its electrochemical performance. Morphologies of electrode materials have remarkable influence on their electrochemical performance. For instance, electrode materials with nanoparticle morphology could enhance the high-rate properties but decrease the volumetric and gravimetric energy density of the electrode and with nanohierarchical morphology can obtain excellent high rate capacity and high tap density [14,15]. Besides, LiCoPO<sub>4</sub> nanoplates have ever been synthesized via a supercritical fluid process [16], but most LiCoPO<sub>4</sub> composites synthesized by the common methods are rod-like or irregular particles [17].

In our recent work, the LiCoPO<sub>4</sub> nanomaterials with a badminton-like morphology were synthesized via hydrothermal method. The electrochemical performance of the synthesized LiCoPO<sub>4</sub> nanobadminton as lithium-ion battery cathode has been studied in detail.

## Experimental

LiOH·H<sub>2</sub>O (≥98.0%), Co(CH<sub>3</sub>COO)<sub>2</sub>·4H<sub>2</sub>O (≥99.0%), (NH<sub>4</sub>)<sub>2</sub>HPO<sub>4</sub> (≥99.0%), NH<sub>3</sub>·H<sub>2</sub>O (25.0 wt.%-28.0 wt.% solution), polyethylene glycol200 (PEG 200) (≥99.7wt.% solution) were all analytical grade and purchased from Chengdu Kelong Chemical Reagent Co., Ltd. The LiCoPO<sub>4</sub> were prepared by a mild hydrothermal synthesis in aqueous solution. The synthesis process was

carried out as follows. At First,  $\text{LiOH}\cdot\text{H}_2\text{O}$ ,  $\text{Co}(\text{CH}_3\text{COO})_2\cdot 4\text{H}_2\text{O}$ , and  $(\text{NH}_4)_2\text{HPO}_4$  were dissolved in water respectively, then  $\text{Co}(\text{CH}_3\text{COO})_2$ , and  $(\text{NH}_4)_2\text{HPO}_4$  solutions were mixed under continuous stirring for several minutes, and  $\text{LiOH}\cdot\text{H}_2\text{O}$  solution,  $\text{NH}_3\cdot\text{H}_2\text{O}$  and PEG 200 were added into above solution one by one. The pH value of the mixed solution were adjusted by using  $\text{NH}_3\cdot\text{H}_2\text{O}$ . All the reagents were added under vigorous stirring. The molar ratio of Li:Co:P was 3:1:1, the concentration of  $\text{Co}^{2+}$  was 0.07M. The as-prepared starting solution was rapidly poured into a stainless autoclave. The autoclave was sealed and maintained at 220 °C for 8 h, and then cooled naturally to room temperature. The product was carefully collected by centrifugation and washed with distilled water and alcohol respectively, and then dried at 40 °C in air overnight. The collected product was set in a tube furnace, heated at a rate 5 °C/min in  $\text{N}_2$  atmosphere, and kept at 350 °C for 2 h, and then continuous heated to 700°C for 8 h to obtain a purple powder for following characterization and measurement. A compare experiment was done by the same process without using PEG 200.

XRD patterns were collected on a Philips X'Pert diffractometer in the  $2\theta$  range 10-80°. Scanning electron microscopy (SEM, JSM-6510LV) was used to analyze the morphological features. Transmission electron microscope (TEM) imaging was carried out on a Tecnai G2F20 S-TWIN scanning TEM (STEM).

The electrochemical performance of the as-prepared samples was evaluated vs a lithium metal anode in coin cells. In a typical experiment, 10 wt.% of the binder PVDF was first dissolved in N-methyl-2pyrrolidone (NMP), and 80 wt.% of active material and 10 wt.% of Acetylene black were subsequently added. This mixture was ground for 30 min to obtain homogeneous slurry, which was then cast on an aluminum foil current collector and dried at 100 °C under vacuum. Coin cells were assembled in an argon-filled glove box. The electrolyte was a mixture of ethylene carbonate (EC) and diethyl carbonate (DEC) in a volume ratio of 1:1 containing  $1.0 \text{ mol dm}^{-3}$   $\text{LiPF}_6$ . A porous polyethylene film (Celgard 2400) was used as a separator. Galvanostatic charge-discharge measurements were performed using automatic charge-discharge equipment (Neware battery testing system BTS-5V/50mA) in a voltage range of 3.0-5.1V at various currents (a rate of 1C corresponded to a current density of  $167 \text{ mA g}^{-1}$ ). Charge-discharge tests were carried out at room temperature.

## Results and Discussion

The XRD patterns of as-synthesized samples are shown in Figure 1. All the reflection peaks can be indexed to an orthorhombic olivine  $\text{LiCoPO}_4$  structure (JCPDS file No. 32-0552). No other impurity phases are found. The diffraction peaks are narrow and sharp. It indicates that well-crystallized pure  $\text{LiCoPO}_4$  can be readily obtained via a hydrothermal reaction.

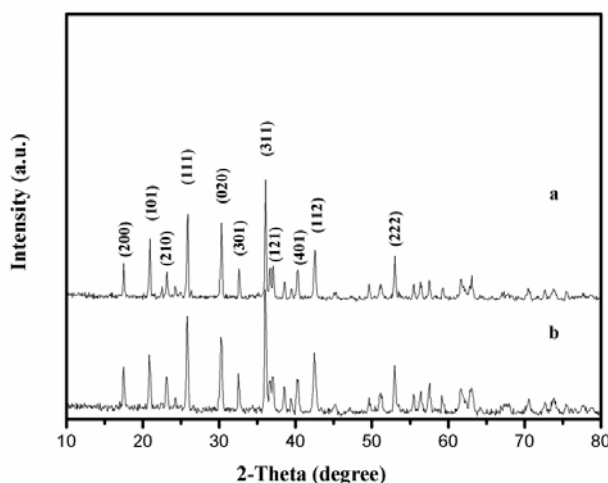


Fig.1 XRD patterns of samples (a) synthesized with PEG200; (b) synthesized without PEG200.

The morphologies of the as-synthesized samples were identified by SEM and TEM. The results are shown in Figure 2. As we can see from Figure 2a, the  $\text{LiCoPO}_4$  synthesized in the presence of PEG 200 have a badminton-like morphology, hierarchical nanobadminton consists of many thin nanorods which are about 200 nm in diameters and 3  $\mu\text{m}$  in length. The morphology of the sample synthesized without adding PEG 200 is made up of lots of aggregated nanoparticles (Figure 2b). The nanoparticles are irregular and have an average diameter of about 500 nm. It indicates that PEG 200 has a significant influence on the morphology of synthesized  $\text{LiCoPO}_4$  nanostructures. For the formation of the  $\text{LiCoPO}_4$  nanobadminton, PEG 200 is believed to play an important role to direct the growth and self-assembly of  $\text{LiCoPO}_4$  nanorods. Figure 2c shows the TEM image of  $\text{LiCoPO}_4$  nanobadminton, and it is consistent with the SEM observation. The tip of a single nanorod is shown in Figure 2d, and the surface of the nanorod is very smooth. Figure 2e and Figure 2f show the HR-TEM images and the selected-area electron diffraction (SAED) pattern of a single nanorod respectively. Interplanar spacings of 2.0208 Å and 2.4369 Å can be attributed to (211) and (231) planes (Figure 2e), the well-defined diffraction spots can be indexed to the [010] zone axis of olivine  $\text{LiCoPO}_4$ , indicating that the nanorod is a single crystalline.

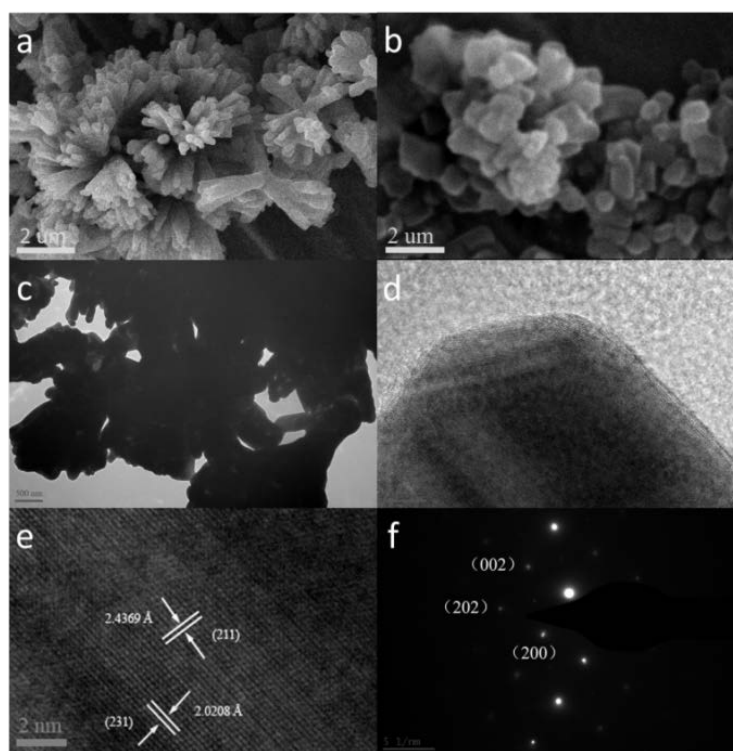


Fig.2 (a) SEM image of sample synthesized with PEG 200; (b) SEM image of sample synthesized without PEG 200; (c) TEM image of sample synthesized with PEG 200; (d), (e) HRTEM image of a single nanorod of nanobadminton synthesized with PEG 200; (f) SAED pattern of a single nanorod of nanobadminton synthesized with PEG 200.

The as-synthesized  $\text{LiCoPO}_4$  nanomaterials were used to act as the cathode materials of lithium ion batteries. The typical charge-discharge curves at 0.1C between 3.0 and 5.1 V (vs  $\text{Li}^+/\text{Li}$ ) are shown in Figure 3. As can be seen, the morphology of  $\text{LiCoPO}_4$  nanomaterials has a great influence on the electrochemical property. Both the two  $\text{LiCoPO}_4$  nanomaterials exhibit a wide and flat voltage plateau at around 4.8 V versus  $\text{Li}^+/\text{Li}$ . The initial discharge capacity of the  $\text{LiCoPO}_4$  nanobadminton can reach  $132.4 \text{ mAhg}^{-1}$ , but the discharge capacity of the  $\text{LiCoPO}_4$  nanoparticles in the first cycle is only  $106.8 \text{ mAhg}^{-1}$ , much lower than that of the nanobadminton. The higher discharge capacity of the  $\text{LiCoPO}_4$  nanobadminton should attribute to its special hierarchical nanostructure of nanorods assembly.

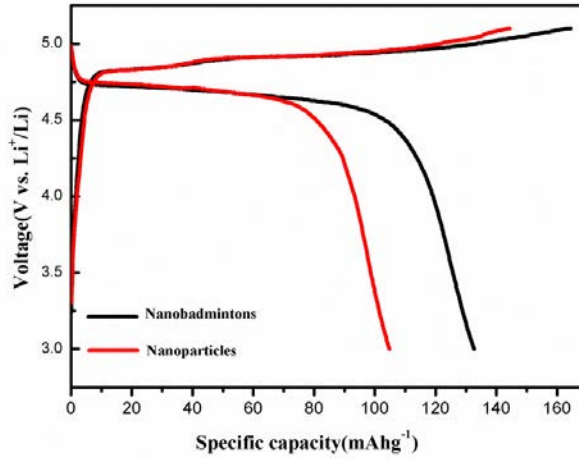


Fig.3 Initial charge-discharge curves of different  $\text{LiCoPO}_4$  electrodes at 0.1C rate.

Figure 4 shows the cycle performance of the  $\text{LiCoPO}_4$ nanobadmintons and nanoparticles as cathodes in lithium-ion batteries. After cycling for 50 times at 0.1C, the capacity of  $\text{LiCoPO}_4$ nanobadmintons is  $99.6\text{mAhg}^{-1}$ , which is much higher than the  $68.1\text{mAhg}^{-1}$  of nanoparticles. The capacity retention of the  $\text{LiCoPO}_4$ nanobadmintons and nanoparticles are 75.2% and 63.8% respectively. The poor cycle stability owing to the instability of electrolyte at 5V. The side reaction between electrolyte and electrode materials may produce a solid electrolyte interface (SEI) layer which will cause the loss of lithium ions [18].

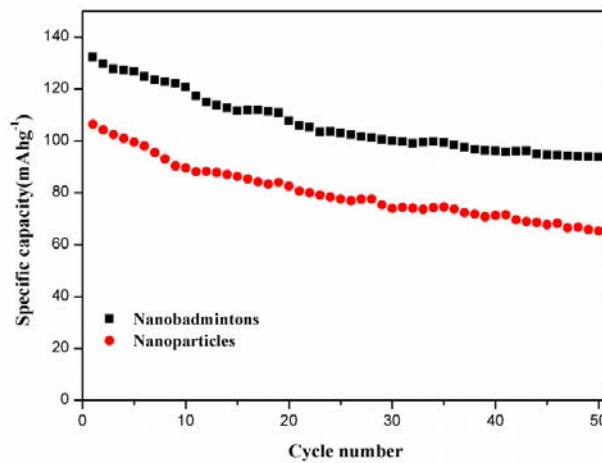


Fig.4 Cycle performance of as-synthesized  $\text{LiCoPO}_4$  electrodes with different morphologies at 0.1C rate.

The rate performance of the  $\text{LiCoPO}_4$ nanobadmintons and nanoparticles at different current densities is shown in Figure 5. As we can see from the Figure 5a, the initial discharge capacities of  $\text{LiCoPO}_4$ nanobadmintons are  $132.4\text{mAhg}^{-1}$ ,  $125.3\text{mAhg}^{-1}$ ,  $113.1\text{mAhg}^{-1}$ ,  $91\text{mAhg}^{-1}$  and  $68.5\text{mAhg}^{-1}$  at the rates of 0.1 C, 0.2 C, 0.5 C, 1 C and 2 C, respectively, while the initial discharge capacities of  $\text{LiCoPO}_4$  nanoparticles are just  $106.8\text{mAhg}^{-1}$ ,  $99.2\text{mAhg}^{-1}$ ,  $85.5\text{mAhg}^{-1}$ ,  $67\text{mAhg}^{-1}$  and  $45.1\text{mAhg}^{-1}$  at the rates of 0.1 C, 0.2 C, 0.5 C, 1 C and 2 C, respectively (Figure 5b). Figure 5c shows the cycle performance of the  $\text{LiCoPO}_4$ nanobadmintons and nanoparticles at different rates. It indicates that the discharge specific capacities of nanobadmintons are higher than those of nanoparticles at all rate conditions. The cycle performance and rate performance of  $\text{LiCoPO}_4$ nanobadmintons are also better than some other reported  $\text{LiCoPO}_4$  nanostructures [19,20].

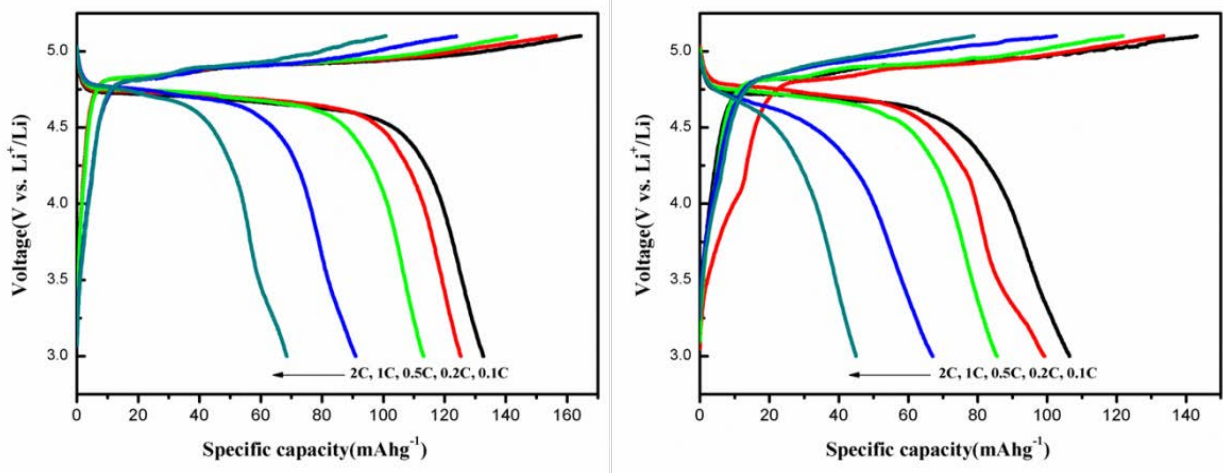
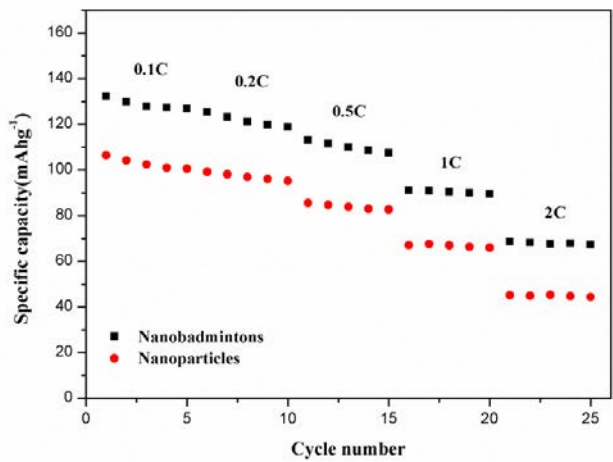


Fig. 5 Charge-discharge curves of LiCoPO<sub>4</sub>nanobadminton (a) and nanoparticles (b) at various rates from 0.1C to 2C.



(c) Reversible capacity of different LiCoPO<sub>4</sub> electrodes during continuous cycling at various discharge rates from 0.1C to 2C.

**Conclusions**

In summary, LiCoPO<sub>4</sub>nanobadminton have been synthesized by a simple hydrothermal method in the presence of PEG 200 and a subsequent high temperature post-annealing process. The initial discharge capacity of LiCoPO<sub>4</sub> nanobadminton at 0.1C can reach 132.4 m Ahg<sup>-1</sup>, which is much better than that of LiCoPO<sub>4</sub> nanoparticles. After 50 cycles, the capacity decrease to 99.6mAhg<sup>-1</sup> and the capacity retention is about 75.2%. The initial discharge capacities of LiCoPO<sub>4</sub>nanobadminton are 125.3mAhg<sup>-1</sup>, 113.1mAhg<sup>-1</sup>, 91mAhg<sup>-1</sup> and 68.5mAhg<sup>-1</sup> at the rates of 0.2C, 0.5C, 1C and 2C, respectively. While the initial discharge capacities of LiCoPO<sub>4</sub> nanoparticles are just 106.8mAhg<sup>-1</sup>, 99.2mAhg<sup>-1</sup>, 85.5mAhg<sup>-1</sup>, 67mAhg<sup>-1</sup> and 45.1mAhg<sup>-1</sup> at the rates of 0.1C, 0.2C, 0.5C, 1C and 2C, respectively. The cycle and rate performance of LiCoPO<sub>4</sub>nanobadminton are better than that of LiCoPO<sub>4</sub> nanoparticles. All these results indicate that LiCoPO<sub>4</sub> nanomaterials with nanobadminton-like morphology are very promising cathode material candidate for lithium-ion batteries.

**Acknowledgments**

This work was supported by the National Natural Science Foundation of China (Grant Nos. 50872084 and 51072124) and Program for New Century Excellent Talents in University (No.

NCET100605). We wish to thank the Analytical & Testing Center of Sichuan University (SCU) for the assistance in sample characterization.

## References

- [1] A.K.Padhi, K.S.Nanjundaswamy, J.B.Goodenough, *J. Electrochem. Soc.* 144 (1997) 1188-1194.
- [2] K. Amine, H. Yasuda, M. Yamachi, *Electrochem. Solid-State Lett.* 3(2000)178-179.
- [3] S.Y. Chung, J.T. Bloking, Y.M. Chiang, *Nat. Mater.* 1 (2002) 123-128.
- [4] J. Wolfenstine, *J. Power Sources* 158 (2006) 1431-1435.
- [5] D. Morgan, A. Van der Ven, G. Ceder, *Electrochem. Solid-State Lett.* 7 (2004) A30-A32.
- [6] R. Sharabi, E. Markevich, V. Borgel, G. Salitra, D. Aurbach, G. Semrau, M.A. Schmidt, N. Schall, C. Stinner, *Electrochem. Commun.* 13 (2011) 800-802.
- [7] R. Sharabi, E. Markevich, K. Fridman, G. Gershinshy, G. Salitra, D. Aurbach, G. Semrau, M.A. Schmidt, N. Schall, C. Bruenig, *Electrochem. Commun.* 28 (2013) 20-23.
- [8] J.L. Allen, T.R. Jow, J. Wolfenstine, *J. Power Sources* 196 (2011) 8656-8661.
- [9] F. Wang, J. Yang, Y.N. NuLi, J.L. Wang, *J. Power Sources* 195 (2010) 6884-6887.
- [10] J. Wolfenstine, J. Read, J.L. Allen, *J. Power Sources* 163 (2007) 1070-1073.
- [11] L. Dimesso, C. Spanheimer, W. Jaegermann, Y. Zhang, A.L. Yarin, *Electrochim. Acta* 95 (2013) 38-42.
- [12] F. Wang, J. Yang, Y.N. NuLi, J.L. Wang, *J. Power Sources* 196 (2011) 4806-4810.
- [13] A. Vadivel Murugan, T. Muraliganth, P.J. Ferreira, A. Manthiram, *Inorg. Chem.* 48 (2009) 946-952.
- [14] X.M. Lou, Y.X. Zhang, *J. Mater. Chem.* 21 (2011) 4156-4160.
- [15] M. Wang, Y. Yang, Y.X. Zhang, *Nanoscale* 3 (2011) 4434-4439.
- [16] Q.C. Truong, M.K. Devaraju, Y. Ganbe, T. Tomai, I. Honma, *Sci. Rep.* 4 (2014) 3975-3982.
- [17] S.T. Sun, C.Q. Du, J.W. Wu, Z.Y. Tang, M. Yang, X.H. Zhang, *Ionics* 20 (2014) 1627-1634.
- [18] L. Dimesso, C. Spanheimer, D. Becker, W. Jaegermann, *J. Eur. Ceram. Soc.* 34 (2014) 933-941.
- [19] L. Dimesso, C. Spanheimer, W. Jaegermann, *J. Power Sources* 243(2013)668-675.
- [20] H.H. Li, Y.P. Wang, X.L. Yang, L. Liu, L. Chen, J.P. Wei, *Solid State Ionics* 255(2014) 84-88.